

Embedded Metal Microstructures in Glass Substrates by a Combined Laser Trenching and Printing Process

Yuval Berg^{1,2}, Shoshana Winter¹, Zvi Kotler¹ and Yosi Shacham-Diamand²

¹ Additive Manufacturing Group, Orbotech Ltd PO Box 215, Yavne 81101, Israel

² Department of Physical Electronics, Faculty of Engineering, Tel Aviv University, Tel Aviv 69978, Israel

E-mail: Yuval.berg@orbotech.com

Control of grooved structured profiles can be achieved by a femtosecond laser ablation process in different materials – dielectrics, semi-conductors and metals. In addition, high accuracy additive manufacturing techniques, e.g. laser induced forward transfer (LIFT), provide flexibility in 3D printed structures deposited on a variety of substrates. The combination of those two laser technologies allows the integration of embedded circuitry and other components, such as microfluidic and micromechanical systems, paving the way to a wide range of applications where conventional subtractive patterning is a problem. Embedding is advantageous in terms of mechanical stability and adherence of the printed metal allowing a favorable aspect ratio and thereby providing improved electrical properties of the conducting lines as well as planar and debris-free surfaces. In this work we report on a combination of laser grooving and laser printing processes and demonstrate the manufacturing of buried copper structures in a grooved borosilicate glass substrate.

DOI: 10.2961/jlmn.2018.02.0013

Keywords: laser induced forward transfer, glass patterning, femtosecond lasers, microelectronics, interposers, interconnects

1. Introduction

Three-dimensional laser micro-fabrication techniques play a key role in modern science and technology, paving the way to emerging interdisciplinary applications. Laser micromachining allows “maskless” fabrication of micro-channels in glass with short turnaround in most substrates, even where conventional subtractive patterning may be difficult, complex and costly [1–3]. Laser patterning can be used for microfluidics applications such as lab-on-chip and in microelectronics for packaging, marking and interconnects to support the rapidly growing mobile system industry. The main requirements are low power consumption and small form factors. Upscale mobile systems also require high speed while simpler internet of things units may use low bandwidth, however, cost is always a factor. It is commonly agreed that interconnects are very often the limiting factor in cost, performance and reliability in most electronic systems; at the chip and packaging levels 3D integrated interconnects can be used to make small form factor systems, reducing capacitance and resistance, hence lowering dynamic power and/or improving performance.

In order to fabricate a 3D structure, several substrate layers need to be processed and integrated. The conventional subtractive fabrication procedure of 3D structures is complex, multi-stepped and its material selection must fit the lithography, etching and cleaning processes [4–6]. Femtosecond (fs) laser-assisted micromachining is a promising alternative technique to produce such 3D structures using transparent dielectric substrates. The 3D capability originates from the nonlinear interaction of femtosecond laser pulses with transparent media. The intensity required

for this highly nonlinear process is achieved by focusing the laser beam inside the dielectric. Ultrashort laser pulses also minimize the heat affected zone allowing the material modification to be controlled and localized on a sub-micrometer scale. The material surrounding the focal volume remains unaffected by the light passing through it, nominally allowing structures to be 3D written at any XYZ coordinate [7–9].

Metal-to-dielectric interfaces are an inherent feature in interconnect systems such as printed circuit boards or multi-level metallization integrated circuits (ICs). While strong metal-dielectric adhesion is required, this can be problematic since the intrinsic adhesion between metallic films and dielectric substrates may be not strong enough and is often inferior to that of metal-to-metal adhesion. One way to improve the metal line integrity is to use embedded structures. Metallizing glasses with fabricated trenches is usually based on trench filling by electrochemical deposition. High aspect ratio trenches can be filled by electroplating deposited on a metal seed that for example can be deposited by electroless plating on a catalytic seed [10,11]. The trench itself can be made by either subtractive patterning or by laser micromachining. For glass metallization, a series of the techniques based on combination of femtosecond laser ablation and femtosecond laser modification assisted electroless plating can fabricate embedded 3D highly conductive microstructures in glass and even closed glass channels with strong adhesion towards biochip and lab-on-a-chip applications, which have been well developed for years [12–15].

Printing of conductive tracks is currently predominated by the printing of nano-metal inks applied by inkjet printing [16,17], screen printing [18] or laser induced forward transfer (LIFT) [19–23]. When using nano-inks, a post-printing sintering step is required to make the printed nano-ink structures conductive. This usually involves significant volume reduction and is therefore not favorable for conformal filling of trenches, cavities or holes. Direct printing of conductive bulk materials as offered by the method of laser induced forward transfer (LIFT) has recently been shown to be a promising approach for producing plastic electronics, printed circuit boards and smart packaging, among many other applications [24].

In this paper, we present a hybrid technique for generating embedded 3D interconnects in glass substrates. The method combines laser trenching of glass by ultrashort pulses followed up by metal printing using the LIFT process. This allows for generation of embedded copper lines and pads in glass with several important advantages: excellent adhesion of micron scale conductive tracks to the glass substrate and significantly reduced lines and spaces with potentially high aspect ratios of the conductive tracks.

2. Experimental setup

Trenching of a 200 μm thick Corning Eagle glass substrate was done by an ultrafast laser (Amplitude Systemes Tangerine HP) with a pulse duration of 270fs at a wavelength of 343nm, with a repetition rate of 175kHz. The pulse energy used was in the regime of 4-10 μJ (slightly above the glass ablation threshold), set by an internal acousto-optic modulator serving as a pulse energy control and also setting an effective repetition rate of 25kHz for the ablation process. A fast galvanometric scanner followed by an F-theta lens (focal length = 100 mm) scans the linearly-polarized, 15 μm Gaussian laser spot on the glass surface.

Printing the copper structures was done using a 532nm laser with 400ps pulse width (Teem Photonics Power Chip), based on the “thermally induced nozzle laser induced forward transfer” (TIN-LIFT) mechanism [25], where jetting of solid copper is used. The laser power is controlled using an acousto-optic modulator. The beam passes through a zoom beam expander. A fixed spot size of 32 μm at the donor interface is used in these experiments. The laser spot is scanned using a fast scanning mirror to control its position and allow patterns to be printed, and the spot is focused onto the donor through an objective lens. Reflected from the scan mirror, the laser beam passes through relay optics before entering the objective in order to keep it in a fixed position at the center of the objective entrance. The donor and acceptor are each positioned on separate xyz translation stages and are held in place by vacuum holders.

The donors are copper donors with a metal thickness of (500 \pm 20) nm, coated on a transparent carrier, and the acceptor is the trenched Eagle glass. The donor is held in its vacuum holder with the transparent layer side up and the laser passes through this layer and focuses on the interface between the transparent and copper layer. Each laser pulse causes the ejection of a single droplet which is propelled towards the acceptor substrate, held at a fixed distance from the donor.

Following the LIFT process the glass is mechanically polished by Buehler Silicon-Carbide grinding paper, type

P4000, to achieve the finest polishing process both to the glass and the printed copper in the trenches, resulting in a smooth uniform surface with the buried conducting lines.

In order to observe the resulting metalized trenches and pads, the glass was grooved at its edges and cut in order to reveal the cross sections of the trenches. The images were studied using a scanning electron microscope (SEM) and optical microscopy.

3. Results and discussion

In the first step, based on the nonlinear absorption of ultrashort pulses in glass, a laser trenching process was developed to produce both lines and pads inside the glass, while controlling the depth and roughness characteristics. Figure 1 depicts cross section SEM images of typical trenches and pads patterned by the femtosecond laser at energies of 6 μJ and 9 μJ per pulse, scanning speed of 20mm/sec and 4 laser scan repeats to deepen the trenches and pads to ~15 μm while maintaining a trench aspect ratio of ~1:1. The pads were patterned at similar laser parameters used for trenches; however, for the pads, multiple overlapping lines at an overlap of 50% (7.5 μm shift from line to line) were used to cover a rectangular shaped pad.

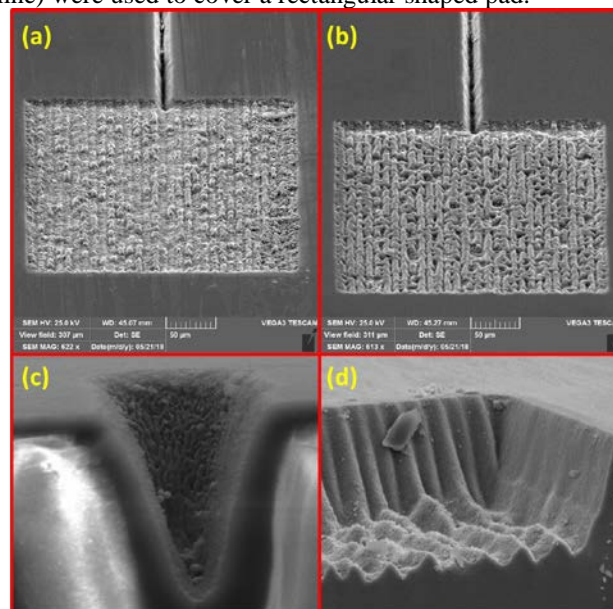


Fig. 1 Patterning in a 200 μm glass: titled SEM image of (a) pad trenched at an energy of 6 μJ per pulse, (b) pad trenched at an energy of 9 μJ per pulse, (c) cross section of a single 15 μm deep trench and (d) corner of a square shaped pad.

The SEM images showed that variations in the laser energy resulted in different surface roughness due to thermal behavior of the ablated glass; at lower energies, slightly above the ablation threshold, one can observe a “cold process” where material is removed, while at higher energies the glass is melted, resulting in smoothed regions. The ablated surface behavior plays a key role in adhesion at the next step of metal printing. There may be a preference to print on a roughened surface, on the scale of the metal droplets (several microns), where adhesion is expected to be superior.

Following the removal of the glass in the patterned regions, copper was printed into the trenches and the pads by the LIFT process. The metal droplets which were printed in

multiple passes result in a structure rising above the glass' surface. The printed copper was then mechanically polished, to ensure that metal lies only underneath the glass surface and that a flat surface is maintained. Following an iterative polish and optical inspection of the copper (and glass), a flat surface with embedded pads and line was achieved. Figure 2 depicts the three-step process that was developed in this work. It should also note that the resulting metal structure showed superior adhesion to the substrate, confirmed by a standard tape test method.

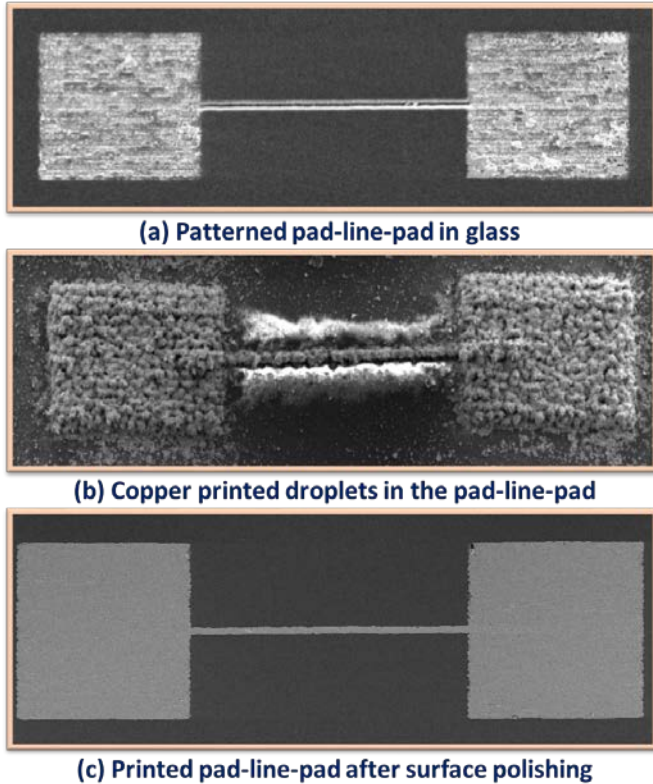


Fig. 2 The three steps process resulting in an embedded printed copper structures in the glass.

Since conduction (electrical resistance) of the metal lines is a key factor, the structure presented (pad-line-pad, e.g. Figure 2c) was examined with a 4-point probe measurement of a 0.5mm copper line. Assuming a triangular shaped trench (see Figure 1c) with a height and depth of $\sim 13\mu\text{m}$, the expected resistance is 0.1Ω . Measurement of several identical lines showed a resistance of $0.5\Omega \pm 5\%$, yielding x5 the bulk copper resistivity. In LIFT printing, lower resistivity of the copper structures typically originates from voids in the printed structure, which depend on the laser fluence and the printing gap [19]. Figure 3 depicts a tilted side view of the corner of a printed pad as seen in SEM after the glass removal.

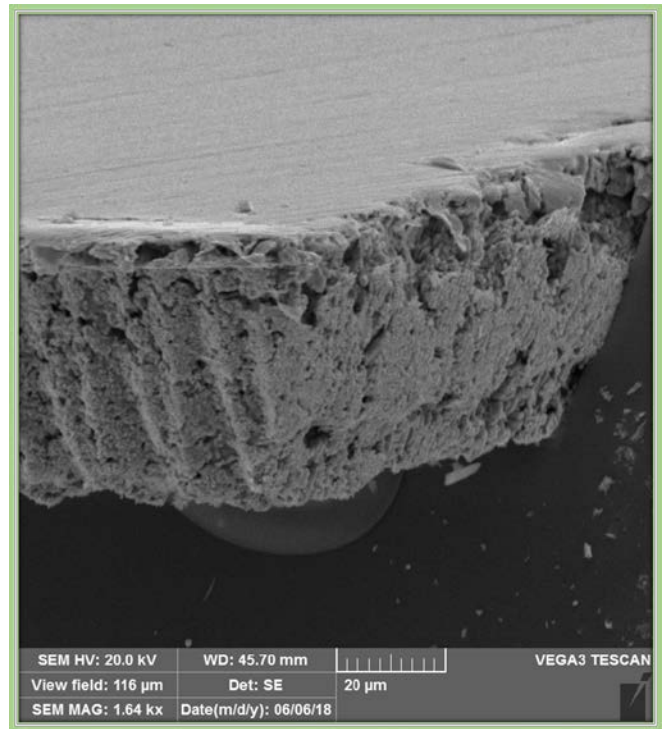


Fig. 3 Tilted cross section SEM image a printed copper pad

By embedding narrow copper lines in the glass, a major challenge in producing glass-based circuitry is overcome, namely that of maintaining its stability. Moreover, it also allows for increasing the line aspect ratio without compromising the stability. On the contrary, embedding thicker lines in the glass trenches increases their adhesion to the substrate, while providing better conductivity. A key factor is the reduced spaces between the lines which are made possible by the trench filling method. Figure 4 shows several parallel printed copper lines with varying spaces between them. The metal filled trenches allow for line spaces which are extremely tight. In this case, the trench (and resulting printed line) width was $14\mu\text{m}$, which is approximately the grooving laser's spot size. Line widths could be easily reduced by decreasing the spot size whenever needed, with the width limitation eventually set by the droplet volume. One can estimate based on previous LIFT printing work that metal lines $<10\mu\text{m}$ could be fabricated in this way [26].

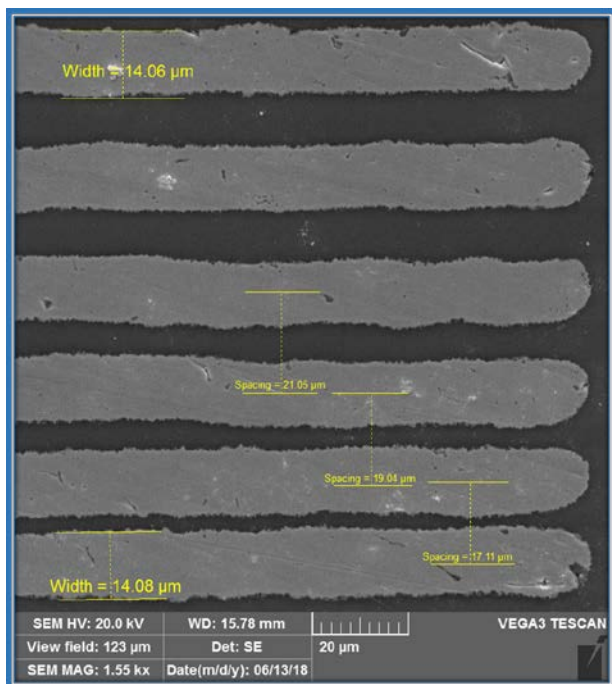


Fig. 4 Varying spaces between the copper filled trenches

While we have demonstrated in this work only copper based circuit elements, there is no fundamental barrier to implement devices made of other materials, using the same method that is demonstrated in this work. Other circuit elements, which involve printed resistive elements as well as other embedded elements, either passive or active, can be implemented by combining laser induced trench formation, LIFT 3D metal deposition and polish planarization.

4. Conclusion

We have demonstrated a novel method for formation embedded metal interconnects in glass substrates. It combines laser trenching of glass by ultrashort pulses and metal printing using the LIFT process. This method is advantageous due to excellent adhesion of micron scale conductive tracks to the glass substrate and significantly reduced line widths and spaces with great potential for high aspect ratio of the conductive tracks.

The method presented in this work can be extended and allow complex circuitry fabrication by embedding multiple materials, i.e., conducting lines, resistors and inductors. It can possibly also be extended to allow fabrication of high density 3D electrical structures in glasses that can serve for example as redistribution layers (RDLs) in advanced electronic packaging applications.

Acknowledgments

This work received funding from the IIA (Israel Innovation Authority), Project No. 60860, "Advanced Laser Technologies for Industries" (ALTIA).

References

- [1] S. Karimelahi, L. Abolghasemi, P.R. Herman, *Appl. Phys. A Mater. Sci. Process.* 114 (2014) 91–111.
- [2] C. Liao, W. Anderson, F. Antaw, M. Trau, *ACS Appl. Mater. Interfaces* (2018) acsami.7b18029.
- [3] Y. Berg, Z. Kotler, Y. Shacham-diamand, J. *Micromechanics Microengineering* 28 (2018)

- aaa780.
- [4] E.J.W. Berenschot, N. Burouni, B. Schurink, J.W. Van Honschoten, R.G.P. Sanders, R. Truckenmuller, H. V. Jansen, M.C. Elwenspoek, A.A. Van Apeldoorn, N.R. Tas, *Small* 8 (2012) 3823–3831.
- [5] H. Ragonés, D. Schreiber, A. Inberg, O. Berkh, G. Kósa, A. Freeman, Y. Shacham-Diamand, *Sensors Actuators, B Chem.* 216 (2015) 434–442.
- [6] C. Lee, C. Chien, C. Chiang, W. Shen, H. Fu, Y. Lee, W. Tsai, P. Chang, C. Zhan, Y. Lin, R. Cheng, C. Ko, W. Lo, Y.L. Rachel, *Microsystems, Packag. Assem. Circuits Technol. Conf.* (2013) 194–197.
- [7] K. Sugioka, Y. Cheng, *Light Sci. Appl.* 3 (2014) e149.
- [8] S. Darvishi, T. Cubaud, J.P. Longtin, *Opt. Lasers Eng.* 50 (2012) 210–214.
- [9] N. Gorodesky, N. Ozana, Y. Berg, O. Dolev, Y. Danan, Z. Kotler, Z. Zalevsky, *J. Opt.* 18 (2016) 095402.
- [10] Y. Shacham-Diamand, V.M. Dubin, *Microelectron. Eng.* 33 (1997) 47–58.
- [11] W. Su, L. Yao, F. Yang, P. Li, J. Chen, L. Liang, *Appl. Surf. Sci.* 257 (2011) 8067–8071.
- [12] J. Xu, Y. Liao, H. Zeng, Z. Zhou, H. Sun, J. Song, X. Wang, Y. Cheng, Z. Xu, K. Sugioka, K. Midorikawa, *Opt. Express* 15 (2007) 12743–12748.
- [13] J. Song, Y. Liao, C. Liu, D. Lin, L. Qiao, Y. Cheng, K. Sugioka, K. Midorikawa, S. Zhang, *J. Laser Micro Nanoeng.* 7 (2012) 334–338.
- [14] J. Xu, D. Wu, Y. Hanada, C. Chen, S. Wu, Y. Cheng, K. Sugioka, K. Midorikawa, *Lab Chip* 13 (2013) 4608–4616.
- [15] J. Xu, H. Kawano, W. Liu, Y. Hanada, P. Lu, A. Miyawaki, K. Midorikawa, K. Sugioka, *Microsystems Nanoeng.* 3 (2016) 1–9.
- [16] E. Tekin, P.J. Smith, U.S. Schubert, *Soft Matter* 4 (2008) 703.
- [17] O. Ermak, M. Zenou, G.B. Toker, J. Ankri, Y. Shacham-Diamand, Z. Kotler, *Nanotechnology* 27 (2016) 385201.
- [18] J. Nijs, E. Demesmaeker, J. Szlufcik, J. Poortmans, L. Frisson, K. De Clercq, M. Ghannam, R. Mertens, R. Van Overstraeten, *Sol. Energy Mater. Sol. Cells* 41–42 (1996) 101–117.
- [19] S. Winter, M. Zenou, Z. Kotler, *J. Phys. D. Appl. Phys.* 49 (2016).
- [20] Y. Berg, M. Zenou, O. Dolev, Z. Kotler, *Opt. Eng.* 54 (2015) 011010.
- [21] L. Yang, C.Y. Wang, X.C. Ni, Z.J. Wang, W. Jia, L. Chai, *Appl. Phys. Lett.* 89 (2006).
- [22] M. Zenou, Z. Kotler, *Opt. Express* 24 (2016) 1431–1446.
- [23] M. Zenou, A. Sa'Ar, Z. Kotler, *Small* 11 (2015) 4082–4089.
- [24] C.B. Arnold, P. Serra, A. Piqué, *MRS Bull.* 32 (2007) 23–32.
- [25] M. Zenou, A. Sa'ar, Z. Kotler, *Sci. Rep.* 5 (2015) 1–10.
- [26] M. Zenou, A. Sa'ar, Z. Kotler, *J. Phys. D. Appl. Phys.* 48 (2015) 205303.

(Received: June 24, 2018, Accepted: September 23, 2018)